# Trans Influence of Phosphines on Dimer−Monomer Interconversion of 2-Pyridinethiolate Complexes: Structures of $[Pd(\mu\text{-}\eta^2\text{-pyS-}N,S)Cl(L)]_2$ (L = $PMe_2Ph$, $PMePh_2$) and $Pd(\eta^2\text{-pyS})Cl(PPh_3)$

**Mukta Gupta, Roger E. Cramer, Kachum Ho, Christina Pettersen, Staffany Mishina, Jack Belli, and Craig M. Jensen***

Department of Chemistry, University of Hawaii, Honolulu, Hawaii 96822

*Received June 23, 1994*[⊗]

The molecular structures of $[Pd(\mu\text{-}\eta^2\text{-pyS-}N,S)Cl(PMe_2Ph)]_2$ (**4**) and $[Pd(\mu\text{-}\eta^2\text{-pyS-}N,S)Cl(PMePh_2)]_2$ (**5**) have been determined by X-ray diffraction. Crystallographic data: for **4**, monoclinic $P2_1/n$, $Z = 4$, $a = 8.952(6)$ Å, $b = 17.665(13)$ Å, $c = 19.288(12)$ Å, $\beta = 95.87(5)°$, $V = 3034(4)$ Å$^3$; for **5**, monoclinic $C2/c$, $Z = 4$, $a = 20.886(10)$ Å, $b = 12.422(6)$ Å, $c = 15.394(14)$ Å, $\beta = 111.62(5)°$, $V = 3713(4)$ Å$^3$. The structural results indicate that there is little variation in the bonding between the pyS ligand and the palladium centers in the dimeric complexes. The molecular structure of $Pd(\eta^2\text{-pyS})Cl(PPh_3)$ (**3**) has been redetermined in a centrosymmetric space group. Crystallographic data: for **3**, triclinic $P\bar{1}$, $Z = 2$, $a = 9.492(4)$ Å, $b = 10.251(6)$ Å, $c = 12.964(8)$ Å, $\alpha = 74.29(5)°$, $\beta = 72.66(4)°$, $\gamma = 65.48(3)°$, $V = 1079.7(10)$ Å$^3$. In solution, complexes **4** and **5** establish equilibria with the corresponding monomer complexes, $Pd(\eta^2\text{-pyS})Cl(PMe_2Ph)$ (**6**) and $Pd(\eta^2\text{-pyS})Cl(PMePh_2)$ (**7**), respectively. While the monomeric complexes are entropically favored, there is an enthalpic preference for the dimeric complexes since coordination of pyS in the bridging mode does not require the severe distortion necessary for chelation of the ligand to a single metal center. The interconversion of **4** and **6** has been studied by variable-temperature $^{31}P\{^1H\}$ NMR spectroscopy. From the changing ratios of the integrated intensities of the signals for **4** and **6** over the 0−70 °C temperature range, values of $\Delta H = 46 \pm 2$ kJ mol$^{-1}$ and $\Delta S = 109 \pm 10$ J K$^{-1}$ mol$^{-1}$ were calculated for the dimer−monomer interconversion. The large positive value observed for $\Delta S$ strongly supports that **4** undergoes reversible dissociation into two monomers. Dilution experiments provide additional verification that the observed dynamic processes involve dimer−monomer interconversions. A shift in equilibrium position toward the monomeric complexes with increasing aryl substitution can be seen through comparison of $^{31}P\{^1H\}$ NMR spectra of equimolar amounts of $[Pd(\mu\text{-}\eta^2\text{-pyS-}N,S)Cl(PMe_3)]_2$ (**1**), **4**, and **5** dissolved in toluene-$d_8$ at 20 °C. Comparison of the energetics determined for the **1**−$Pd(\eta\text{-pyS})Cl(PMe_3)$ (**2**) and **4**−**6** equlibria indicates that this shift is due to the decreasing values of $\Delta H$ upon aryl substitution of the phosphines. It is concluded that the differing values for the $\Delta H$ for the dimer−monomer equilibria arise from strengthened Pd−N interactions resulting from the decreased donor ability of the trans aryl-substituted phosphines in the monomeric complexes.

## Introduction

Recently, there have been several reports of 2-pyridinethiolate,(pyS) complexes which exhibit dynamic behavior in solution.[1−3] Variable-temperature solution NMR and boiling point elevation (molecular weight determination) studies[3] have shown that, in solution, the complex $[Pd(\mu\text{-}\eta^2\text{-pyS-}N,S)Cl(PMe_3)]_2$ (**1**) establishes a rapid equilibrium with the monomeric chelate complex $Pd(\eta^2\text{-pyS})Cl(PMe_3)$ (**2**) as seen in eq 1. By contrast, it was recently reported by Nakamura *et al.*[4] that the closely related complex $Pd(\eta^2\text{-pyS})Cl(PPh_3)$ (**3**) is a stable monomer in solution. In order to elucidate the reasons for the differing stabilities of **1** and **3**, we have prepared the mixed alkyl−aryl phosphine complexes $[Pd(\mu\text{-}\eta^2\text{-pyS-}N,S)Cl(PMe_2Ph)]_2$ (**4**) and $[Pd(\mu\text{-}\eta^2\text{-pyS-}N,S)Cl(PMePh_2)]_2$ (**5**) and studied their solution dynamics. Additionally, we have determined the structures of **4** and **5** and redetermined the structure of **3** through single-crystal X-ray diffraction studies.

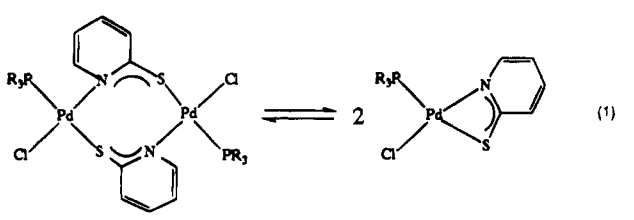


(1)

## Experimental Section

**General Details.** The following were purchased and used without further purification: 2-pyridinethiol, triphenylphosphine (Aldrich Chemical Co.) dimethylphenylphosphine, and methyldiphenylphosphine (Strem Chemicals Inc.). The complexes $[PdCl(PMe_2Ph)(\mu\text{-}Cl)]_2$, $[PdCl(PMePh_2)(\mu\text{-}Cl)]_2$, and $[PdCl(PPh_3)(\mu\text{-}Cl)]_2$ were prepared using a method analogous to Chatt and Venanzi's synthesis of $[PdCl(PEt_3)(\mu\text{-}Cl)]_2$.[5] The complexes **1**[4] and **3**[4] were prepared by literature methods.

The $^1H$ NMR and $^{31}P$ NMR spectra were recorded on a GN omega 500 spectrometer at 500.1 and 202.4 MHz, respectively. The $^1H$ NMR data are listed in ppm downfield from TMS at 0.00 ppm. $^{31}P$ NMR chemical shifts were measured relative to the deuterium resonance of

[⊗] Abstract published in *Advance ACS Abstracts,* December 1, 1994.

(1) Deeming, A. J.; Meah, M. N.; Bates, P. A.; Hursthouse, M. B. *J. Chem. Soc., Dalton Trans.* **1988**, 2193−2199.
(2) Ciriano, M. A.; Viguri, F.; Torrente-Perez, J. J.; Lahoz, F. J.; Oro, L. A.; Tiripicchio, A.; Tiripicchio-Camellini, M. J. *J. Chem. Soc., Dalton Trans.* **1990**, 25−32.
(3) Yamamoto, J. H.; Yoshida, W.; Jensen, C. M. *Inorg. Chem.* **1991**, *30*, 1353−1357.
(4) Nakatsu, Y.; Matsumoto, K.; Ooi, S.; Nakamura, Y. *Inorg. Chim. Acta* **1992**, *196*, 81−88.
(5) Chatt, J.; Venanzi, L. M. *J. Chem. Soc.* **1957**, 2351−2356.

0020-1669/95/1334-0060$09.00/0 

**Table 1.** Summary of Crystal Data for Complexes **4**, **5**, and **3**

| | **4** | **5** | **3** |
|---|---|---|---|
| formula | $Pd_2C_{26}H_{30}N_2P_2S_2Cl_2$ | $Pd_2C_{36}H_{34}N_2P_2S_2Cl_2$ | $PdC_{23}H_{19}NPSCl$ |
| fw | 780.3 | 904.5 | 514.3 |
| cryst dimens, $mm^3$ | 0.2 × 0.3 × 0.4 | 0.1 × 0.2 × 0.2 | 0.3 × 0.2 x 0.1 |
| cryst system | monoclinic | monoclinic | triclinic |
| space group | $P2_1/n$ | $C2/c$ | $P\bar{1}$ |
| $a$, Å | 8.952 (6) | 20.886 (10) | 9.492 (4) |
| $b$, Å | 17.665 (13) | 12.422 (6) | 10.251 (6) |
| $c$, Å | 19.288 (12) | 15.394 (14) | 12.964 (8) |
| α, deg | 90.00 | 90.00 | 74.29 (5) |
| $\beta$, deg | 95.87 (5) | 111.62 (5) | 72.66 (4) |
| $\gamma$, deg | 90.00 | 90.00 | 65.48 (3) |
| $V$, $Å^3$ | 3034 (4) | 3713 (4) | 1079.7 (10) |
| Z | 4 | 4 | 2 |
| $\rho_{calc}$, $g/cm^3$ | 1.708 | 1.622 | 1.582 |
| $\lambda$, Å (Mo Kα radiation) | 0.71073 | 0.71073 | 0.71073 |
| $T$, K | 297 | 297 | 297 |
| scan type | $\omega$ | $\omega$ | $2\theta-\theta$ |
| scan rate, deg/min | 1.50−15.00 | 1.50−15.00 | 1.50−15.00 |
| $2\theta$ range, deg | 4.0−40.0 | 4.0−40.0 | 3.0−50.0 |
| $\mu$, $mm^{-1}$ | 1.604 | 1.323 | 1.147 |
| min−max transm coeff | 0.3626−0.4293 | 0.8025−0.9471 | 0.6087−0.7436 |
| no. of reflns collected | 3227 | 3833 | 4074 |
| no. of indept reflns | 2848 | 1749 | 3822 |
| no. of unique data with $I > 3\sigma(I)$ | 2176 | 1243 | 3092 |
| $R$,[a] % | 2.80 | 3.14 | 2.84 |
| $R_w$,[b] % | 3.31 | 3.52 | 2.84 |
| goodness of fit[c] | 1.16 | 1.16 | 2.16 |

[a] $R = \Sigma||F_o| - |F_c||/\Sigma F_o$. [b] $R_w = [w\Sigma(|F_o| - |F_c|)^2/\Sigma wF_o^2)]^{1/2}$. [c] GOF $= [\Sigma w(|F_o| - |F_c|)^2/(N_o - N_v)]^{1/2}$.

the solvent by using the internal frequency lock of the spectrometer so that the resonance from a capillary of 85% $H_3PO_4$, centered in a 5 mm NMR tube containing the deuterated solvent, appeared at 0.0 ppm at 20 °C. A preacquisition delay of 1 s and a pulse delay of 0.82 s were used in the variable-temperature $^{31}P$ NMR experiments.

**Preparation of [Pd($\mu$-$\eta^2$-pyS-*N*,*S*)Cl(PMe$_2$Ph)]$_2$ (4).** An ethanolic solution of sodium ethoxide under nitrogen (prepared by dissolving 0.025 g (1.105 mmol) of sodium in 40 mL of absolute ethanol) is treated with 2-pyridinethiol (0.112 g, 1.00 mmol). Under nitrogen purge, [PdCl(PMe$_2$Ph)($\mu$-Cl)]$_2$ (0.315 g, 0.500 mmol) is added to the clear, yellow solution arising upon completion of the heterocyclic deprotonation, and the resulting suspension is allowed to stir for 24 h. The resulting air-stable orange solid is isolated by filtration from the reaction mixture. The product is extracted with 10 mL of dicholoromethane, and the residual NaCl is separated from the mixture by filtration. The microcrystalline, orange product is isolated upon removal of the dichloromethane under vaccum followed by recrystallization from toluene (0.323 g, 73.6% yield). $^1H$ NMR (dicholoromethane-$d_2$, −60 °C): $\delta$ 8.48 (2H, m), 7.97 (4H, m), 7.48 (6H, m), 7.33 (2H, d), 7.21 (2H, m), 6.88 (2H, t) (aromatic); 2.07 (6H, d, $J_{P-H}$ = 13 Hz) ($PCH_3$), 1.55 (6H, d, $J_{P-H}$ = 12 Hz) ($PCH_3$). $^{31}P\{^1H\}$ NMR (toluene-$d_8$, −50 °C): $\delta$ 8.7 (s).

**Preparation of [Pd($\mu$-$\eta^2$-pyS-*N*,*S*)Cl(PMePh$_2$)]$_2$ (5).** An ethanolic solution of sodium ethoxide under nitrogen (prepared by dissolving 0.03 g (1.305 mmol) of sodium in 40 mL of absolute ethanol) is treated with 2-pyridinethiol (0.115 g, 1.05 mmol). Under nitrogen purge, [PdCl(PMePh$_2$)($\mu$-Cl)]$_2$ (0.3795 g, 0.503 mmol) is added to the clear, yellow solution arising upon completion of the heterocyclic deprotonation, and the resulting suspension is allowed to stir for 48 h. The resulting air-stable reddish orange solid is isolated by filtration from the reaction mixture. The product is extracted with 10 mL of dicholoromethane, and the residual NaCl is removed by filtration. The microcrystalline, orange product is isolated upon removal of the dichloromethane under vaccum followed by recrystallization from toluene (0.3489 g, 76.7% yield).

**Crystallographic Studies.** Crystals suitable for X-ray diffraction were obtained by slow evaporation of toluene solutions. The crystals of **3**−**5** were mounted on glass fibers with epoxy. The crystals of **4** and **5** were centered on a Nicolet P3 and the crystal of **3** was centered on a Nicolet P1 automated diffractometer. The unit cell parameters were obtained by least-squares refinement of the setting angles of 20 reflections. Crystal and instrument stabilities were monitored with a set of three standard reflections measured every 97 reflections; in all cases no significant variations were found. Ellipsoidal semiempirical absorption corrections were applied for all three data sets. Crystal data and relevant information for **4**, **5**, and **3** are summarizied in Table 1.

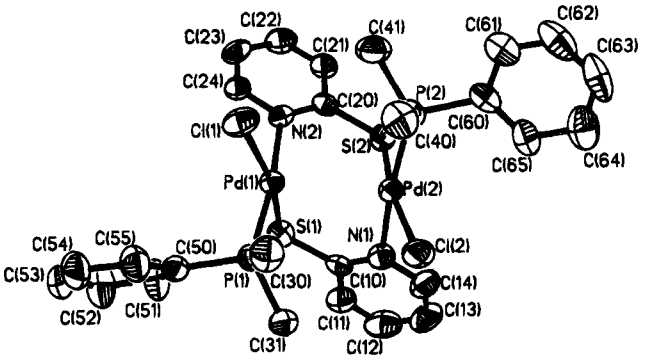


**Figure 1.** Diagram of [Pd($\mu$-$\eta^2$-pyS-*N*,*S*)Cl(PMe$_2$Ph)]$_2$ (**4**). Thermal ellipsoids are at 50% probability. The hydrogen atoms have been omitted for clarity.

The structures were solved by direct methods using SHELX PLUS computer programs (Nicolet instrument Corp.) and refined by full-matrix least-squares procedures. All non-hydrogen atoms were refined with anisotropic temperature coefficients. The hydrogen atoms were included by use of a riding model with C−H distances of 0.96 Å and isotropic thermal parameters fixed at 0.08 $Å^2$.

## Results

**Structures of [Pd($\mu$-$\eta^2$-pyS-*N*,*S*)Cl(PMe$_2$Ph)]$_2$ (4) and [Pd($\mu$-$\eta^2$-pyS-*N*,*S*)Cl(PMePh$_2$)]$_2$ (5).** The new dipalladium pyS complexes **4** and **5** were synthesized by the method previously reported for the synthesis of the $PMe_3$ complex, **1**. The molecular structures of **4** and **5** were determined by single-crystal X-ray diffraction studies. Diagrams of the obtained structures with the atomic numbering schemes are seen in Figures 1 and 2. Selected bond angles and distances are listed in Tables 2 and 3. The final fractional atomic coordinates are given in Tables 4 and 5.

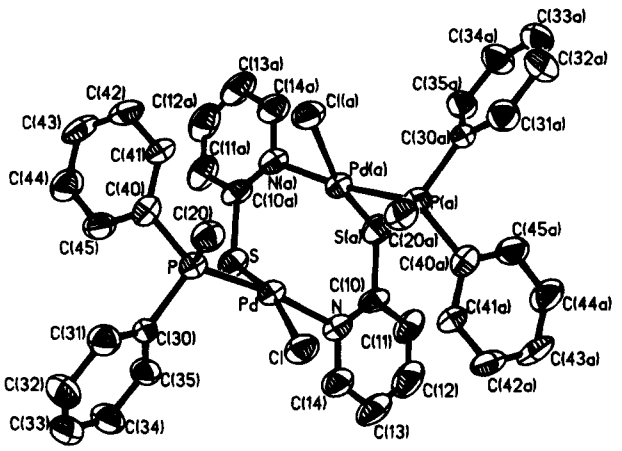


**Figure 2.** Diagram of $[Pd(\mu\text{-}\eta^2\text{-pyS-}N,S)Cl(PMePh_2)]_2$ (**5**). Thermal ellipsoids are at 50% probability. The hydrogen atoms have been omitted for clarity.

The molecular structure of **4** has approximate $C_2$ symmetry, while $C_2$ symmetry is crystallographically imposed on **5**. The two palladium atoms of both structures are linked through two $\mu$-pyS ligands in a head-to-tail fashion. The coordination geometry about each of the palladium atoms is nearly square planar. The chlorine atoms are oriented trans to the sulfur of the bridging ligand, while the phosphines are oriented trans to nitrogen. No significant differences are observed in the interatomic distances between the palladium center and corresponding donor atoms in **4** and **5**. The Pd−Pd distances of 2.921(2) and 2.982(3) Å for **4** and **5**, respectively, clearly demonstrate the lack of Pd−Pd bonding in these complexes. The N−C−S angles of 122.9(5) and 123.1(6)° for **4** and 121.9(5)° for **5** are nearly idealized for $sp^2$ carbons. The S−C bond distances of 1.732(7) and 1.735(7) Å in **4** and 1.775(9) Å in **5** are within the 1.72−1.80 Å range which has been found[1-3,6-8] in pyS complexes and indicate that the bridging pyS ligands have a significant amount of thione character.

**Structure of $Pd(\eta^2\text{-pyS})Cl(PPh_3)$ (3).** An X-ray structure determination of **3** was previously carried out by Nakamura *et al.*[4] They reported a noncentrosymmetric, triclinic unit cell containing two symmetry-independent monomers. The monomers are chemically equivalent but have major differences in bond distances, a condition which has been associated with the presence of an overlooked center of symmetry.[9] We found the same unit cell as previously reported.[4] However, we were able to redetermine the structure in the centrosymmetric space group $P\bar{1}$, in which the two monomers in the unit cell are related by a center of symmetry. Refinement of our 3−50° data set in $P\bar{1}$ converged at $R = 0.0284$ and $R_w = 0.0284$ while values of $R = 0.044$ and $R_w = 0.067$ were obtained for the 3−50° data set previously reported in $P1$ by Nakamura *et al.* A diagram of the obtained structure with the atomic numbering scheme is seen in Figure 3. Selected bond angles and distances are listed in Tables 2 and 3. The final fractional atomic coordinates are given in Table 6.

The coordination geometry about the palladium atom is nearly square planar. The chlorine atom is oriented trans to the sulfur of the pyS ligand while the phosphine is oriented trans to the nitrogen of the pyS ligand. The pyS ligand forms a four-membered chelate ring with the palladium atom. The S−C−N angle of 109.0(3)° is severely distorted from the nearly idealized trigonal angles found in the dimeric complexes **4** and **5**. This result is in agreement with the S−C−N angles of 109−115° which have been observed for pyS ligands chelated to a monometal center.[8] The Pd−S bond distance of 2.297(2) Å is not significantly different from the 2.296(3) and 2.285(3) Å distances in **4** and the 2.287(3) Å distance in **5**. However, the 2.092(3) Å Pd−N bond distance is significantly shorter than the 2.124(6) and 2.131(7) Å distances in **4** and the 2.131(7) Å distance in **5**. The S−C bond distance of 1.743(4) Å is within the 1.72−1.80 Å range which has been found[1-3,6-8] in pyS complexes and indicates that the pyS ligand has a significant amount of thione character.

**NMR Studies.** Variable-temperature NMR studies and boiling point elevation experiments have shown[3,10] that the dimers **1**, $[Pd(\mu\text{-}\eta^2\text{-pyrimidine-2-thiolate-}N,S)Cl(PMe_3)]_2$ (**8**), and $[Pd(\mu\text{-}\eta^2\text{-methylpyrimidine-2-thiolate-}N,S)Cl(PMe_3)]_2$ (**9**) establish temperature-dependent equilibria with the corresponding monomer complexes in solution. Variable-temperature $^{31}P\{^1H\}$ NMR spectra were obtained for a solution of 0.006 mmol of **4** dissolved in 0.5 mL of toluene-$d_8$. As seen in Figure 4, **4** establishes dimer−monomer equilibria in solution similar to those observed for **1**, **8**, and **9**. At 0 °C, sharp resonances are observed at 8.2 and 6.7 ppm for **4** and the corresponding monomer complex, $Pd(\eta^2\text{-pyS})Cl(PMe_2Ph)$ (**6**), respectively. At this temperature, the dimeric complex clearly dominates the equilibrium. As the temperature is raised, the signals gradually broaden with the increasing rate of dimer−monomer interconversion. Also the relative intensity of **6** rapidly increases with increasing temperature. Thus, while the dimer−monomer equilibrium ratio is 8.1:1 at 0 °C, the ratio is 0.6:1 at 70 °C. Upon cooling, the trend was reversed and spectra identical to those initially obtained were observed with no loss of integrated intensity with an equal number of acquisitions. From the changing ratios of the integrated intensities of the two signals over the range 0−70 °C, values of $\Delta H = 46 \pm 2$ kJ mol$^{-1}$ and $\Delta S = 109 \pm 10$ J K$^{-1}$ mol$^{-1}$ for the dimer−monomer interconversion were calculated. The large positive value observed for $\Delta S$ strongly supports that **4** undergoes reversible dissociation into two monomers. Dilution experiments provide additional verification that the observed dynamic processes involve dimer−monomer interconversions. The **4**−**6** equilibrium position shifts from the 2.2:1 intensity ratio of the upfield to downfield resonances observed for a solution of 0.0045 mmol of **4** in 0.5 mL of toluene-$d_8$ to a 0.6:1 ratio observed upon 5-fold dilution. A parallel experiment with **1** shows a shift in dimer−monomer ratio from 3.4:1 to 1:1 upon 5-fold dilution. These results precludes the possibility that the observed dynamic processes involve dimer−dimer interconversion since dilution would not affect the equilibrium position of such processes. The

(6) (a) Deeming, A. J.; Meah, M. N.; Dawes, H. M.; Hursthouse, M. B. *J. Organomet. Chem.* **1986**, *299*, C25−C28. (b) Deeming, A. J.; Meah, M. N.; Bates, P. A.; Hursthouse, M. B. *J. Chem. Soc., Dalton Trans.* **1988**, 235−238. (c) Deeming, A. J.; Karim, M.; Bates, P. A.; Hursthouse, M. B. *Polyhedron* **1988**, *7*, 1401−1403.

(7) Ciriano, M. A.; Viguri, F.; Torrente-Perez, J. J.; Lahoz, F. J.; Oro, L. A.; Tiripicchio, A.; Tiripicchio-Camellini, M. J. *J. Chem. Soc., Dalton Trans.* **1990**, 1493−1502.

(8) (a) Fletcher, S. R.; Skapski, A. C. *J. Chem. Soc., Dalton Trans.* **1972**, 635−639. (b) Cotton, F. A.; Fanwick, P. E.; Fitch, J. W. *Inorg. Chem.* **1978**, *17*, 3254−3257. (c) Masaki, M.; Matsunami, S.; Ueda, H. *Bull. Chem. Soc. Jpn.* **1978**, *51*, 3298−3301. (d) Mura, P.; Olby, B. G.; Robinson, S. D. *J. Chem. Soc., Dalton Trans.* **1985**, 2101−2112. (e) Rosenfield, S. G.; Swedberg, S. A.; Arora, S. K.; Mascharak, P. K. *Inorg. Chem.* **1986**, *25*, 2109−2114. (f) Rosenfield, S. G.; Berends, H. P.; Gelmini, L.; Stephan, D. W.; Mascharak, P. K. *Inorg. Chem.* **1987**, *26*, 2792−2797. (g) Deeming, A. J.; Hardcastle, K. I.; Meah, M. N.; Bates, P. A.; Dawes, H. M.; Hursthouse, M. B. *J. Chem. Soc., Dalton Trans.* **1988**, 227−233. (h) Deeming, A. J.; Meah, M. N.; Randle, N. P.; Hardcastle, K. I. *J. Chem. Soc., Dalton Trans.* **1989**, 2211−2216.

(9) (a) Jones, P. G. *Chem. Soc. Rev.* **1984**, *13*, 157−172. (b) Baur, W. H.; Tillmanns, E. *Acta Crystallogr.* **1986**, *B42*, 95−111. (c) Marsh, R. E.; Herbstein, *Acta Crystallogr.* **1983**, *B39*, 280−287.

(10) Yap, P. A.; Jensen, C. M. *Inorg. Chem.* **1992**, *31*, 4823−4828.

**Table 2.** Comparison of Selected Bond Distances (Å) for Complexes **1**, **4**, **5**, and **3**

| 1 | | 4 | | 5 | | 3 | |
|---|---|---|---|---|---|---|---|
| Pd(1)−N(2) | 2.131(9) | Pd(1)−N(2) | 2.124(6) | Pd−N | 2.131(7) | Pd−N | 2.092(3) |
| Pd(2)−N(1) | 2.131(8) | Pd(2)−N(1) | 2.131(7) | | | | |
| Pd(1)−S(1) | 2.284(3) | Pd(1)−S(1) | 2.296(3) | Pd−S | 2.287(3) | Pd−S | 2.297(2) |
| Pd(2)−S(2) | 2.306(3) | Pd(2)−S(2) | 2.285(3) | | | | |
| Pd(1)−P(1) | 2.243(4) | Pd(1)−P(1) | 2.233(3) | Pd−P | 2.243(3) | Pd−P | 2.239(2) |
| Pd(2)−P(2) | 2.244(3) | Pd(2)−P(2) | 2.239(3) | | | | |
| Pd(1)−Cl(1) | 2.356(3) | Pd(1)−Cl(1) | 2.353(3) | Pd−Cl | 2.351(3) | Pd−Cl | 2.352(2) |
| Pd(2)−Cl(2) | 2.355(3) | Pd(2)−Cl(2) | 2.352(3) | | | | |

**Table 3.** Comparison of Selected Bond Angles (deg) for Complexes **1**, **4**, **5**, and **3**

| 1 | | 4 | | 5 | | 3 | |
|---|---|---|---|---|---|---|---|
| S(1)−Pd(1)−P(1) | 89.3(1) | S(1)−Pd(1)−P(1) | 90.9(1) | S−Pd−P | 92.9(1) | S−Pd−P | 98.1(1) |
| S(2)−Pd(2)−P(2) | 91.6(1) | S(2)−Pd(2)−P(2) | 88.6(1) | | | | |
| Cl(1)−Pd(1)−N(2) | 90.1(3) | Cl(1)−Pd(1)−N(2) | 90.7(2) | Cl−Pd−N | 90.7(2) | Cl−Pd−N | 98.2(1) |
| Cl(2)−Pd(2)−N(1) | 90.0(2) | Cl(2)−Pd(2)−N(1) | 88.8(2) | | | | |
| Cl(1)−Pd(1)−P(1) | 90.4(1) | Cl(1)−Pd(1)−P(1) | 88.9(1) | Cl−Pd−P | 85.9(1) | Cl−Pd−P | 93.0(1) |
| Cl(2)−Pd(2)−P(2) | 89.7(1) | Cl(2)−Pd(2)−P(2) | 92.2(1) | | | | |
| S(1)−Pd(1)−N(2) | 88.3(2) | S(1)−Pd(1)−N(2) | 88.0(2) | S−Pd−N | 89.6(2) | S−Pd−N | 70.3(1) |
| S(2)−Pd(2)−N(1) | 88.0(2) | S(2)−Pd(2)−N(1) | 89.1(2) | | | | |
| P(1)−Pd(1)−N(2) | 172.8(3) | P(1)−Pd(1)−N(2) | 173.3(2) | P−Pd−N | 172.7(2) | P−Pd−N | 166.7(1) |
| P(2)−Pd(2)−N(1) | 176.9(2) | P(2)−Pd(2)−N(1) | 173.5(2) | | | | |
| S(1)−Pd(1)−Cl(1) | 164.3(1) | S(1)−Pd(1)−Cl(1) | 167.4(1) | S−Pd−Cl | 165.6(1) | S−Pd−Cl | 168.1(1) |
| Cl(2)−Pd(2)−S(2) | 167.2(1) | Cl(2)−Pd(2)−S(2) | 168.7(1) | | | | |
| Pd(1)−S(1)−C(11) | 114.7(4) | Pd(1)−S(1)−C(10) | 114.5(3) | Pd−S−C(10A) | 111.5(3) | Pd−S−C(10) | 81.3(2) |
| Pd(2)−S(2)−C(21) | 113.9(4) | Pd(2)−S(2)−C(20) | 114.0(3) | | | | |
| Pd(1)−N(2)−C(25) | 115.1(8) | Pd(1)−N(2)−C(24) | 115.9(5) | Pd−N−C(14) | 114.9(7) | Pd−N−C(10) | 99.1(2) |
| Pd(2)−N(1)−C(15) | 117.5(7) | Pd(2)−N(1)−C(14) | 116.6(5) | | | | |
| Pd(1)−N(2)−C(21) | 124.1(7) | Pd(1)−N(2)−C(10) | 124.6(5) | Pd−N−C(10) | 128.2(5) | Pd−N−C(14) | 138.9(4) |
| Pd(1)−N(2)−C(11) | 125.2(6) | Pd(1)−N(2)−C(20) | 125.5(4) | | | | |
| S(1)−C(11)−N(1) | 123.2(7) | S(1)−C(10)−N(1) | 123.1(6) | N−C(10)−SA | 121.9(6) | N−C(10)−S | 109.0(3) |
| S(2)−C(21)−N(2) | 124.5(8) | S(2)−C(20)−N(2) | 122.9(5) | | | | |
| C(11)−N(1)−C(15) | 116.9(8) | C(14)−N(1)−C(10) | 118.0(7) | C(10)−N(2)−C(14) | 116.8(7) | C(10)−N−C(14) | 121.2(4) |
| C(21)−N(2)−C(25) | 119.8(9) | C(24)−N(2)−C(20) | 118.5(6) | | | | |
| S(1)−C(11)−C(12) | 116.8(8) | S(1)−C(10)−C(11) | 116.4(6) | C(11)−C(10)−S(a) | 115.4(8) | C(11)−C(10)−S | 130.9(4) |
| S(2)−C(21)−C(22) | 116.1(9) | S(2)−C(20)−C(21) | 117.1(6) | | | | |

dilution experiments also indicate that, at equal concentration and temperature, there is a shift in equilibrium position toward monomer upon aryl substitution.

$^{31}P\{^1H\}$ NMR spectroscopic studies of a solution of 0.0009 mmol of **5** dissolved in 0.5 mL of toluene-$d_8$ show that the $PMePh_2$ complex also establishes dimer−monomer equilbria in solution. At 20 °C, a ratio of 0.5:1 is observed for the integrated intensities of the resonances for **5** and Pd($\eta^2$-pyS)Cl($PMePh_2$) (**7**) at 24 and 20 ppm, respectively. At −60 °C, a 1.6:1 dimer: monomer ratio is observed. Thus the equilibrium position between **5** and **7** follows the trends noted for the **4**−**6** and **1**−**2** equilibria: a shift toward dimer with decreasing temperature and a shift toward monomer with increasing aryl substitution. Unfortunately, the energetics of the interconversion of **5** and **7** could not be determined since the low solubility of **5** makes the required variable-temperature NMR study impractical.

Unlike the case of the trialkyl and mixed alkyl−aryl phosphine complexes, a single sharp resonance is observed by $^{31}P\{^1H\}$ NMR for the triphenylphosphine complex, **3**, at 20 °C.[4] The possibility that **3** is in equilibrium with the corresponding dimer is virtually precluded by our observation of a single sharp resonance at 31 ppm over the temperature range −80 to +20 °C. Thus **3** must have greater stability than the $PMe_3$, $PMe_2Ph$, and $PMePh_2$ monomers **2**, **6**, and **7**.

## Discussion

The dimer−monomer equilibria observed for the $PMe_3$, $PMe_2Ph$, and $PMePh_2$ complexes **1**, **4**, and **5**, respectively, can be explained in terms of two thermodynamic considerations. The first is the simple entropic preference for the monomeric complexes. The second is the severe geometric distortion of the pyS ligand which is required for its chelation to a single metal center. This distortion is perhaps best illustrated by the S−C−N angles of 109−115° which have been found[8] in such monomeric chelating pyS complexes. By contrast, nearly idealized S−C−N angles of 117−124° have been found[2,3,7] for the bridging pyS ligands. Our structural results are in accordance with these trends. At low temperatures, the unstrained dimeric form of the complexes is preferred. As the temperature is raised, the equilibria are entropically driven toward the monomeric complexes.

Our structural data show no significant differences in the Pd−N or Pd−S bond distances in **4** and **5**. Thus aryl substitution of the phosphine ligand has little effect on the coordinative interaction of the pyS ligand in the dimeric palladium complexes. This is in agreement with the earlier analysis[3,10] of the structures of **1**, **8**, and **9**, which found that the interaction between the nitrogens of rigid six-membered 2-thiaheterocycles and the palladium centers is geometrically rather than electronically limited.

A reaction coordinate diagram for the dimer−monomer interconversions at 20 °C is seen in Figure 5. Since the coordinative interactions in the dimer complexes are invariant, it can be assumed that they lie at approximately the same energy. The energies of the Pd($\eta^2$-pyS)ClL monomers are ordered in accordance with the equilibrium positions observed for equal

**Table 4.** Atomic Coordinates and Equivalent Isotropic Displacement Coefficients[a] for $[Pd(\mu\text{-}\eta^2\text{-pyS-}N,S)Cl(PMe_2Ph)]_2$ (**4**)

| atom | x | y | z | $U_{eq}$, Å$^2$ |
|---|---|---|---|---|
| Pd(1) | 0.1200(1) | 0.2114(1) | 0.6118(1) | 0.035(1) |
| Pd(2) | 0.3487(1) | 0.1857(1) | 0.7287(1) | 0.037(1) |
| Cl(2) | 0.5153(2) | 0.2887(1) | 0.7298(1) | 0.054(1) |
| S(2) | 0.2105(2) | 0.0807(1) | 0.7488(1) | 0.047(1) |
| S(1) | −0.0304(2) | 0.2418(1) | 0.6972(1) | 0.048(1) |
| Cl(1) | 0.2249(2) | 0.1824(1) | 0.5080(1) | 0.056(1) |
| P(2) | 0.5010(2) | 0.1120(1) | 0.6729(1) | 0.046(1) |
| C(40) | 0.6090(9) | 0.1629(5) | 0.6138(4) | 0.060(3) |
| C(41) | 0.4230(9) | 0.0360(5) | 0.6174(5) | 0.070(4) |
| P(1) | 0.1656(2) | 0.3337(1) | 0.5936(1) | 0.042(1) |
| C(30) | 0.3414(8) | 0.3533(5) | 0.5581(4) | 0.059(3) |
| C(31) | 0.1697(10) | 0.3966(4) | 0.6677(4) | 0.056(3) |
| N(2) | 0.0525(6) | 0.0969(3) | 0.6218(3) | 0.035(2) |
| N(1) | 0.2140(7) | 0.2498(3) | 0.7923(3) | 0.044(3) |
| C(24) | −0.0439(8) | 0.0696(5) | 0.5689(4) | 0.045(3) |
| C(20) | 0.0894(8) | 0.0521(4) | 0.6777(4) | 0.037(3) |
| C(21) | 0.0280(8) | −0.0208(4) | 0.6802(4) | 0.046(3) |
| C(10) | 0.0660(9) | 0.2620(4) | 0.7776(4) | 0.038(3) |
| C(23) | −0.1088(8) | 0.0001(5) | 0.5700(4) | 0.049(3) |
| C(22) | −0.0701(9) | −0.0463(4) | 0.6271(5) | 0.054(3) |
| C(53) | −0.2171(11) | 0.4155(5) | 0.4356(5) | 0.065(4) |
| C(50) | 0.0178(9) | 0.3683(4) | 0.5306(4) | 0.043(3) |
| C(13) | 0.1993(13) | 0.2983(5) | 0.9080(5) | 0.073(4) |
| C(11) | −0.0193(10) | 0.2925(4) | 0.8284(5) | 0.058(3) |
| C(14) | 0.2782(10) | 0.2690(4) | 0.8566(5) | 0.060(4) |
| C(52) | −0.2452(10) | 0.3936(6) | 0.5003(5) | 0.079(4) |
| C(65) | 0.7284(9) | 0.1140(5) | 0.7811(5) | 0.058(3) |
| C(51) | −0.1283(10) | 0.3704(5) | 0.5481(5) | 0.066(4) |
| C(12) | 0.0478(13) | 0.3100(5) | 0.8922(5) | 0.074(5) |
| C(60) | 0.6366(9) | 0.0687(5) | 0.7375(4) | 0.049(3) |
| C(55) | 0.0436(10) | 0.3903(5) | 0.4644(5) | 0.062(4) |
| C(54) | −0.0740(12) | 0.4134(5) | 0.4172(5) | 0.070(4) |
| C(61) | 0.6500(10) | -0.0092(5) | 0.7453(5) | 0.063(4) |
| C(64) | 0.8326(10) | 0.0838(6) | 0.8315(5) | 0.077(4) |
| C(63) | 0.8451(11) | 0.0070(7) | 0.8371(6) | 0.083(5) |
| C(62) | 0.7538(13) | -0.0382(6) | 0.7952(6) | 0.083(5) |

[a] Equivalent isotropic $U$ defined as one-third of the trace of the orthogonalized $\mathbf{U}_{ij}$ tensor.

**Table 5.** Atomic Coordinates and Equivalent Isotropic Displacement Coefficients[a] for $[Pd(\mu\text{-}\eta^2\text{-pyS-}N,S)Cl(PMePh_2)]_2$ (**5**)

| atom | x | y | z | $U_{eq}$, Å$^2$ |
|---|---|---|---|---|
| Pd | 0.0087(1) | 0.1779(1) | 0.3506(1) | 0.039(1) |
| Cl | 0.0799(1) | 0.3227(2) | 0.4262(1) | 0.052(1) |
| S | −0.0594(1) | 0.0278(2) | 0.3141(2) | 0.052(1) |
| P | −0.0793(1) | 0.2824(2) | 0.3493(1) | 0.041(1) |
| N | 0.0966(3) | 0.0795(5) | 0.3708(5) | 0.047(3) |
| C(31) | −0.0984(4) | 0.3888(8) | 0.4993(6) | 0.051(4) |
| C(33) | −0.0745(5) | 0.3097(9) | 0.6490(6) | 0.057(4) |
| C(30) | −0.0756(4) | 0.2953(7) | 0.4684(5) | 0.039(4) |
| C(10) | 0.1129(4) | 0.0251(7) | 0.3062(6) | 0.046(4) |
| C(34) | −0.0512(5) | 0.2181(8) | 0.6203(6) | 0.059(5) |
| C(40) | −0.1674(4) | 0.2413(7) | 0.2842(6) | 0.046(4) |
| C(32) | −0.0980(4) | 0.3937(8) | 0.5888(7) | 0.055(5) |
| C(41) | −0.1966(5) | 0.2582(8) | 0.1873(6) | 0.055(4) |
| C(35) | −0.0508(4) | 0.2109(7) | 0.5319(6) | 0.049(4) |
| C(44) | −0.2742(5) | 0.1605(8) | 0.2763(7) | 0.069(5) |
| C(45) | −0.2067(4) | 0.1907(7) | 0.3276(6) | 0.056(4) |
| C(11) | 0.1700(5) | −0.0413(8) | 0.3292(8) | 0.065(5) |
| C(43) | −0.3021(4) | 0.1800(8) | 0.1821(7) | 0.067(5) |
| C(14) | 0.1395(5) | 0.0687(7) | 0.4602(7) | 0.060(5) |
| C(13) | 0.1980(5) | 0.0057(9) | 0.4868(8) | 0.075(5) |
| C(42) | −0.2625(5) | 0.2279(8) | 0.1391(6) | 0.060(5) |
| C(12) | 0.2115(5) | −0.0508(9) | 0.4193(10) | 0.082(6) |
| C(20) | −0.0762(4) | 0.4194(6) | 0.3067(5) | 0.048(4) |

[a] Equivalent isotropic $U$ defined as one-third of the trace of the orthogonalized $\mathbf{U}_{ij}$ tensor.

concentration solutions at 20 °C. Since the equilibrium favors the monomer complexes when L = $PMe_3$ and $PMe_2Ph$, they must lie at the energies higher than the dimers, with the $PMe_3$ monomer at the higher energy since its equilibrium is more in favor of the dimer complex. The L = $PMePh_2$ complex is at lower energy than the dimer since, in this case, the equilibrium is monomer dominated. The observed shift in the dimer−monomer equilibrium toward the monomer Pd($\eta^2$-pyS)ClL complexes upon increasing aryl substitution culminates with the $PPh_3$ complex, **3**, which is stabilized to the extent that the corresponding dimer is not observed. Thus, it can be assumed that it lies at the lowest energy relative to the dimer complexes.

Comparison of the energetics determined[11] for the **1**−**2** and **4**−**6** equilibria reveals that both $\Delta H$ and $\Delta S$ decrease upon aryl

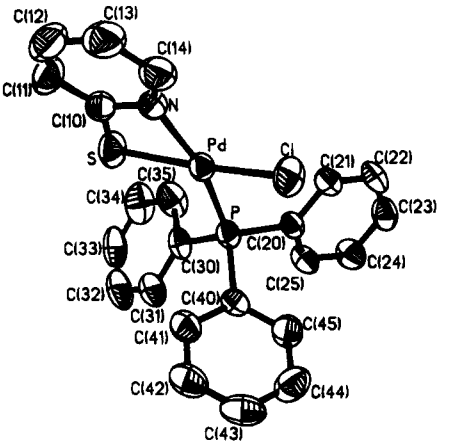


**Figure 3.** Diagram of Pd($\eta^2$-pyS)Cl($PPh_3$) (**3**). Thermal ellipsoids are at 50% probability. The hydrogen atoms have been omitted for clarity.

**Table 6.** Atomic Coordinates and Equivalent Isotropic Displacement Coefficients[a] for Pd($\eta^2$-pyS)Cl($PPh_3$) (**3**)

| atom | x | y | z | $U_{eq}$, Å$^2$ |
|---|---|---|---|---|
| Pd | 0.1149 (1) | 0.3847 (1) | 0.1973 (1) | 0.040 (1) |
| Cl | 0.3152(1) | 0.2041(1) | 0.2919(1) | 0.039(1) |
| S | 0.2756(1) | 0.5428(1) | 0.1718(1) | 0.061(1) |
| P | −0.0284(1) | 0.2722(1) | 0.2162(1) | 0.061(1) |
| N | −0.0519(3) | 0.5323(3) | 0.1329(2) | 0.046(2) |
| C(21) | 0.5799(4) | 0.2106(4) | 0.1238(3) | 0.048(2) |
| C(14) | −0.1116(5) | 0.6732(5) | 0.0925(3) | 0.062(2) |
| C(10) | −0.1397(5) | 0.4472(5) | 0.1603(3) | 0.053(2) |
| C(20) | 0.5247(4) | 0.1397(4) | 0.2260(3) | 0.039(2) |
| C(30) | 0.2719(4) | 0.0382(4) | 0.3354(3) | 0.047(2) |
| C(22) | 0.7396(5) | 0.1621(5) | 0.0768(3) | 0.059(2) |
| C(35) | 0.2802(5) | −0.0286(5) | 0.2521(4) | 0.068(2) |
| C(25) | 0.6310(4) | 0.0213(4) | 0.2779(3) | 0.052(2) |
| C(32) | 0.1983(5) | −0.1514(5) | 0.4662(4) | 0.075(3) |
| C(31) | 0.2302(4) | −0.0240(4) | 0.4433(3) | 0.057(2) |
| C(11) | −0.2943(5) | 0.5064(6) | 0.1457(4) | 0.072(3) |
| C(12) | −0.3550(6) | 0.6505(7) | 0.1045(4) | 0.084(3) |
| C(40) | 0.3022(4) | 0.2666(3) | 0.4136(3) | 0.040(2) |
| C(41) | 0.1554(5) | 0.3077(4) | 0.4868(3) | 0.053(2) |
| C(23) | 0.8445(5) | 0.0469(5) | 0.1305(3) | 0.059(2) |
| C(42) | 0.1360(5) | 0.3666(5) | 0.5759(3) | 0.064(2) |
| C(45) | 0.4262(5) | 0.2883(4) | 0.4316(3) | 0.056(2) |
| C(24) | 0.7922(5) | −0.0255(4) | 0.2316(3) | 0.059(2) |
| C(43) | 0.2600(6) | 0.3875(5) | 0.5932(4) | 0.070(2) |
| C(33) | 0.2096(5) | −0.2166(5) | 0.3844(5) | 0.075(3) |
| C(44) | 0.4048(5) | 0.3491(5) | 0.5212(4) | 0.071(3) |
| C(34) | 0.2492(5) | −0.1554(5) | 0.2776(5) | 0.080(3) |
| C(13) | −0.2650(6) | 0.7368(6) | 0.0767(4) | 0.079(3) |

[a] Equivalent isotropic $U$ defined as one-third of the trace of the orthogonalized $\mathbf{U}_{ij}$ tensor.

(11) Incorrect values for the energetics of the **1**−**2** equilibrium process were reported in ref 3. The reported values were determined using erroneous equilibrium constants which were calculated at a point when it was still assumed that the dynamic process involved a dimer−dimer rather than a dimer−monomer equilibrium. The true equilibrium constants lead to the the corrected calculated values of $\Delta H = 52 \pm 2$ kJ mol$^{-1}$ and $\Delta S = 122 \pm 10$ J K$^{-1}$ mol$^{-1}$.

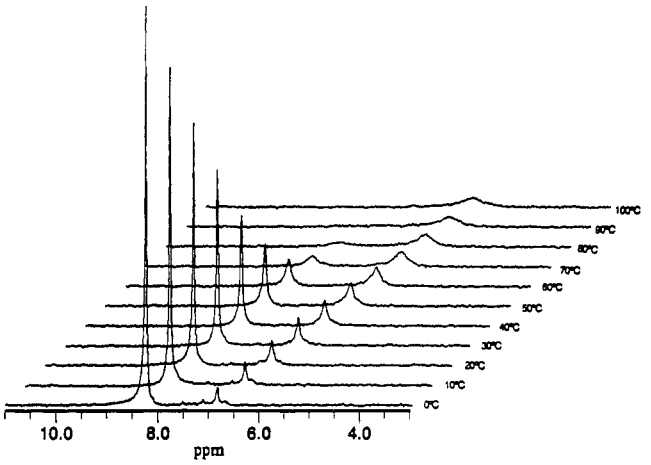


**Figure 4.** Variable-temperature $^{31}P\{^1H\}$ NMR spectra (202.4 MHz) of 0.006 mmol of $[Pd(\mu\text{-}\eta^2\text{-pyS-}N,S)Cl(PMe_2Ph)]_2$ (**4**) dissolved in 0.5 mL of toluene-$d_8$.

substitution. Thus the relative shift in the **4**−**6** equilibria toward the monomer is due to the decreasing value of $\Delta H$ since a decrease in $\Delta S$ favors the dimer. We find no significant differences in the bond distances between the pyS ligands and the palladium centers in the dimer complexes. Also very limited steric interactions are seen between the phosphine and pyS ligands in both the monomer and dimer complexes. In the monomer complex **3**, the $PPh_3$ ligand and the aromatic ring of the pyS ligand are transoid, thus precluding steric interaction. While the phoshine ligands of the dimer complexes are cisoid to the aromatic ring of one pyS ligand, little steric congestion arises since the planes of these rings are perpendicular to the Pd-P axes. Thus the differing values for the $\Delta H$ for the dimer−monomer equilibria must result from variation in the pyS bonding interactions in the monomer complexes. This is possibly due to strengthened Pd−N interactions resulting from the decreased donor ability of the trans aryl-substituted phosphines. The presence of a stronger Pd−N interaction in **3** is supported by the Pd−N bond distance of 2.092(3) Å in **3**. This distance is significantly shorter than the Pd−N distances of 2.137(9) and 2.131(8) Å found[3] for **1**, 2.124(6) and 2.131(7) Å found for **4**, and 2.131(7) Å found for **5**. It is noteworthy that **8** and **9** which have Pd−N distances of 2.143(3) and 2.120(2) Å, respectively, establish rapid dimer−monomer equilibria while $[Pd(\mu\text{-}\eta^2\text{-methylimidazole-2-thiolate-}N,S)Cl(PMe_3)]_2$, which has Pd−N distances of 2.092(7) and 2.096(7) Å, exhibits no dynamic behavior.[10]

## Conclusion

This work demonstrates the delicate balance of energetic factors which influence the stability and interconversion of the dimer $[Pd(\mu\text{-}\eta^2\text{-pyS-}N,S)Cl(L)]_2$ and monomer $Pd(\eta^2\text{-pyS})Cl(L)$ complexes. While the monomers are entropically favored, there is an enthalpic preference for the dimers since coordination of pyS in the bridging mode does not require the severe distortion necessary for chelation of the ligand to a single metal center. Our results indicate that increasing aryl substitution of the trimethylphosphine results in strengthening of the Pd−N interaction in the monomeric pyS complexes, culminating in the stabilized monomer complex **3**.

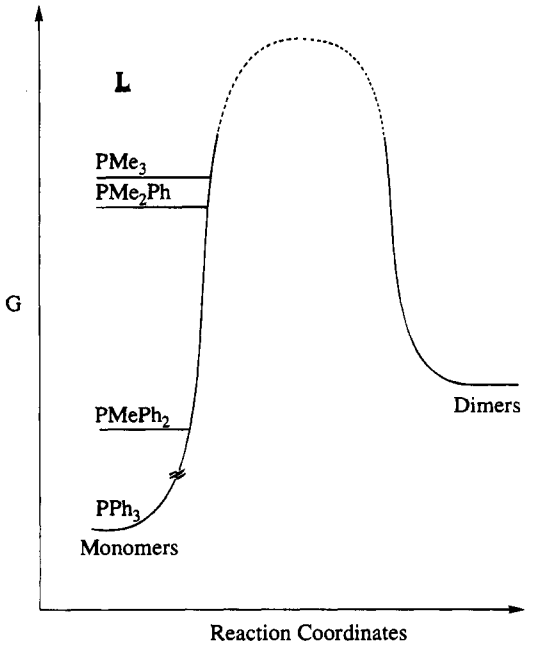


**Figure 5.** Reaction coordinate diagram of the interconversion of $[Pd(\eta^2\text{-pyS})Cl(L)]_2$ and $Pd(\eta^2\text{-pyS})Cl(L)$ at 20 °C.

**Acknowledgment.** We thank the University of Hawaii Research Council for support of this research. We thank Ms. Elizabeth DeFeo for helpful discussions. The assistance of Mr. W. Yoshida for the NMR spectroscopic studies is gratefully acknowledged.

**Supplementary Material Available:** A table and plot of variable-temperature NMR data, along with calculations of energetics, and tables of anisotropic thermal parameters, bond distances, bond angles, hydrogen atom coordinates, and isotropic thermal parameters for $[Pd(\mu\text{-}\eta^2\text{-pyS-}N,S)Cl(PMe_2Ph)]_2$ (**4**), $[Pd(\mu\text{-}\eta^2\text{-pyS-}N,S)Cl(PMePh_2)]_2$ (**5**), and $Pd(\eta^2\text{-pyS})Cl(PPh_3)$ (**3**) (19 pages). Ordering information is given on any current masthead page.

IC940731Y